

On the Horopter and Hering-Hillebrand Deviation

Fredrik Bergholm

CVAP, NADA, KTH
S-100 44 Stockholm, Sweden

Antônio Francisco

Inst. Nacional de Pesquisas Espaciais/LAC
São José dos Campos, São Paulo, Brazil

Abstract

We discuss the usage of Hering-Hillebrand deviation H in depth perception, be it machine vision or human vision.

1. Background

In building an efficient machine vision system equipped with binocular vision, there is much to be learnt from human vision. In psychophysics, ophthalmology, and related sciences there is more than a century of accumulated knowledge or experience.

The underlying idea behind our work is that **asymmetry** should be an integrated part of a visual binocular system, be it machine vision or human vision. Asymmetry, is not a quirk of a binocular system, but a very sensible property if it is to be used for sensing relative depth in an efficient way. In machine vision, where people have neglected to introduce asymmetry, some artificial distortions arise.

Having described basic notation and concepts, we will introduce the idea of *linear correspondence* upon which our binocular analysis is based. The next section reviews some concepts on horopters, as a preparation for the theory in Sec.4. Using that theory, we discuss strategies for letting corresponding points vary with fixation distance, in Sec. 5. Section 6 discusses perception of planarity with *modified disparity*, exemplified by computer vision experiments.

1.1 Stereo in General – our View

The old theory on the horopter, as developed by Ogle and Ames at the Dartmouth Eye Institute (1929-1947) at Hanover, New Hampshire, see [1],[2],[3], deviates in certain respects from the one to be presented below. (See also [4].) The motivation for using conic sections, for describing the human longitudinal horopter, was according to Ogle purely empirical.

We look upon the state of affairs in a slightly different manner. For several reasons, an asymmetric stereo system seems apriori to be preferable (to be developed, below) to a symmetric one. Given that, we may pose the question: What is the simplest theoretical arrangement for creating any asymmetric correspon-

dence between rays in the left and right eye? This, theoretically derived “horopter” turns out to essentially coincide with the empirical one. In other words, from our point of view, the theoretical and empirical horopters are the same thing, and there is no real need to think of deviations between the geometric and theoretical horopter, as is customary.

The family of conic sections introduced by Ogle (1932), for measuring the empirical longitudinal horopter, contains two parameters: the so-called *Hering-Hillebrand deviation H* and a constant R_0 dealing with unequal magnification in the two eyes. We show what values of H are suitable from a theoretical standpoint, given that the visual system attempts to sense depth from horizontal disparities simultaneously avoiding perceiving planar surfaces as nonplanar. Such an analysis reveals that H should be implemented so that it *varies* with fixation distance. Such a dependence of H with distance has also, partly, been observed empirically by Ogle.

Although there has been much discussion on whether corresponding retinal points are stable or not when varying fixation distance, it has not been sufficiently stressed that stability of corresponding points is not really a desirable property, in the first place, for a binocular system. In fact, we show that whereas an elliptical-like horopter is good for close distances, say within distances of a couple of metres from the eyes, the Vieth-Müller circle is the reasonable choice beyond 5–6 m.

2. Correspondence of Rays

Used notation for binocular geometry runs as follows. There are two pinhole “camera” coordinate systems, called L and R , the x_L, y_L, z_L -system and the x_R, y_R, z_R -system, and also a world coordinate system, called W , (with orthogonal coordinate frame), the coordinates of which are denoted x, y, z .

Let the projection centre of L (left camera) expressed in world coordinates be $A = (-b/2, 0, 0)$ and that of R (right camera) be $B = (b/2, 0, 0)$. Let the unit vectors of L be $\vec{e}_{1L}, \vec{e}_{2L}, \vec{e}_{3L}$ and those of R be

$\vec{e1}_R, \vec{e2}_R, \vec{e3}_R$, and assume they are expressed in the world coordinate system with origin at the midpoint of the baseline AB. The length of the baseline is b . The directions $\vec{e3}_L, \vec{e3}_R$ will point in the directions of the *optical axes*. If there are image planes involved, they will be spanned by $\vec{e1}_L, \vec{e2}_L$ (=left image plane) and $\vec{e1}_R, \vec{e2}_R$ (=right image plane). However, since our main theme is correspondences between rays, image surfaces will mostly play a subordinate rôle. In machine vision they would typically be planar since CCD sensor arrays are planar (in current technology), and in human vision, spherical-like.

The coordinates of L and R , expressed in W , are consequently: $(x, y, z) = (-b/2, 0, 0) + x_L \cdot \vec{e1}_L + y_L \cdot \vec{e2}_L + z_L \cdot \vec{e3}_L$, or, $(x, y, z) = (b/2, 0, 0) + x_R \cdot \vec{e1}_R + y_R \cdot \vec{e2}_R + z_R \cdot \vec{e3}_R$.

We assume that the z_L - and z_R -axes, i.e. $\vec{e3}_R$ and $\vec{e3}_L$, intersect at a *fixation point* P . We also assume there is no torsion, whereby we mean that the fixation plane is spanned by the four vectors $\vec{e3}_L, \vec{e1}_L, \vec{e3}_R, \vec{e1}_R$, all lying in the fixation plane (=visual plane). The z -coordinate of the fixation point P is denoted by z_0 , and will be called *fixation distance*.

The only unorthodox feature of the binocular geometry we will introduce is that of *asymmetry*, cf. Fig. 1. Whereas, normally, an optical axis is (for good reasons) perpendicular to the x -axis of an image plane, i.e. $\vec{e1}_L \perp \vec{e3}_L$ or $\vec{e1}_R \perp \vec{e3}_R$, we will in our analysis, from time to time, assume the contrary¹: $\vec{e1}_L \not\perp \vec{e3}_L$ or $\vec{e1}_R \not\perp \vec{e3}_R$. To be crystal clear about this: When using $\vec{e1}_L \perp \vec{e3}_L$, we use x_L^\perp, z_L^\perp instead of x_L, z_L , also adding a superscript, replacing $\vec{e1}_L$ by $\vec{e1}_L^\perp$. Analogously for x_R, z_R , and $\vec{e1}_R$.

2.1 The Idea of Linear Correspondence

Considering characteristics of human vision, the word 'camera' in the introduced binocular model, should be replaced by 'eye'. We use (like Ogle) the pinhole model of image formation for crudely explaining binocular correspondences in human vision. This pinhole can be thought of as the mean nodal point of each eye, if one so wishes. Although we use a pinhole camera model, we do not delete the lens altogether in our model, in the sense we assume that $\vec{e3}_L$ or $\vec{e3}_R$ is the optical axis of a thick lens *perpendicular* to an image plane (image tangent plane) in the fovea spanned by $\vec{e1}_L^\perp, \vec{e2}_L^\perp$ or $\vec{e1}_R^\perp, \vec{e2}_R^\perp$, otherwise quite blurry images would arise, cf. Scheimpflug's condition.

What is the simplest conceivable correspondence relation between rays in L and R ? Well, a **linear correspondence** defined by saying that **the ray represented by the axis $z_L = k \cdot x_L$ correspond to**

the ray represented by the axis $z_R = k \cdot x_R$, if and only if, the k -values are equal. If $(x_L, z_L) = (x_L^\perp, z_L^\perp)$ are used, the wellknown Vieth-Müller circles arise, *but* if $\vec{e1}_L \not\perp \vec{e3}_L$ etc., then a conic is the curve formed by intersecting corresponding rays. This can be proved, rewriting $z_L/x_L = z_R/x_R = k$ expressed in (x, y, z) -coordinates, yielding **a conic** in the (x, z) -plane:

$$(x, z, 1)C(x, z, 1)^T = 0 \quad (1)$$

where C is a 3 by 3 matrix and T is transpose. We have, in fact, shown: *If 'nature' constructs binocular ray correspondences as simply as possible, it either chooses sections of circles or conics (e.g. ellipses).*

3. On Human Vision

There are various techniques² for measuring the *empirical* curve of corresponding rays in human vision, the horopter, extensively described in a book by Ogle (1964), and in several articles, for example Ogle (1932). We refer the reader to this literature, for more detailed descriptions and discussions on horopters. Since there are many kinds of horopters, a small clarification is in place. We primarily consider a class of horopters called *longitudinal horopters*, where measurements are made by making people observe short vertical rods (or half-rods) in various positions, adjustable along lanes in depth. In this class of horopters, we are mainly interested in those determined from either of the criteria: (a) center of space region where rods are binocularly fused, (b) equal subjective directions. The first criterion is more like asking people when they perceive zero disparity, and the second when the upper half of a rod only visible to the left eye coincides with the lower part only visible to the right eye, blocking the eyes in this way.

For symmetric fixation, see Fig. 1, Ogle recommended the use of the following horopter:

$$\cot \alpha_L - \cot \alpha_R = H \quad (2)$$

$$\iff \frac{z_L^\perp}{x_L^\perp} - \frac{z_R^\perp}{x_R^\perp} = H \quad (3)$$

which is a *conic* since Eq. 3 is a conic in (x, z) -coordinates for much the same reason that $x_L/z_L = x_R/z_R$ is a conic in Eq. 1. The parameter H in Eq. 2 is called Hering-Hillebrand deviation. See also App. A. Experimentally, $H \approx 0.10$ at a distance of $z_0 = 40$ cm, but $H \approx 0.05$ at $z_0 = 76$ cm, Ogle (1964, Table 3, p.34).

¹The notation $\not\perp$ means 'not perpendicular to'.

²Locus of intersection of equal subjective directions, Ogle(1964, pp.12-14). Locus of fused rods.

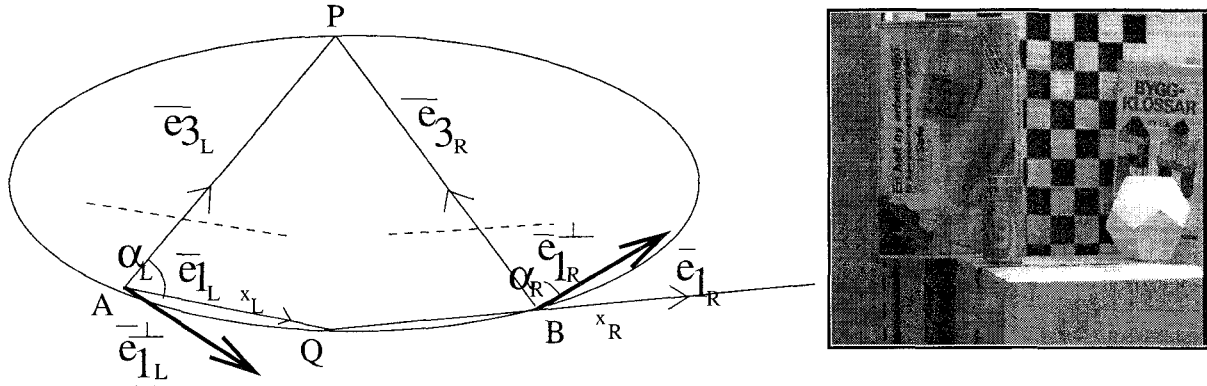


Figure 1: (a) Curve of corresponding rays = elliptical horopter. P = fixation point. AP , BP are fixation rays. AQ , BQ are associated directions. Associated image planes are dashed.(b) Used image (left) in Sec.6.

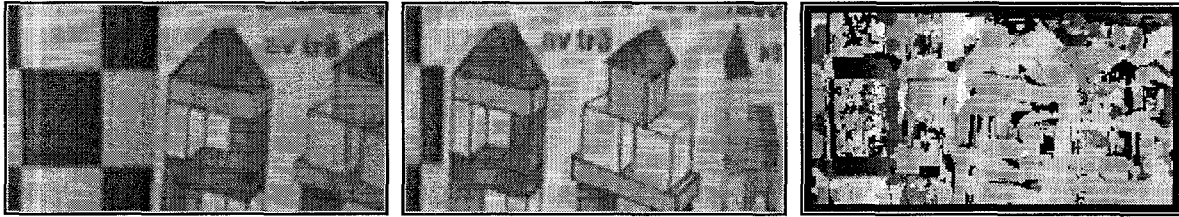


Figure 2: Convergent binocular geometry: Left = left image (subset of Fig. 1), Middle = right image, Right = Horizontal disparity image $d(x, y)$. Motif: Box occluding periodic checker board pattern.

Ogle looked upon conics as a means for *approximating* horopters. He did not motivate the use of conics, the way we do. Instead, Ogle (1932; pp. 672-679), did this as follows. Empirically, “horopters” (criterion=apparent frontoparallel plane) studied earlier by Hering, Helmholtz and others tended to be concave at near, become flat at some observation distance, called *abathic distance*, and convex toward the observer for greater distances. Ogle wanted to construct a *family* of horopters depending on fixation distance z_0 such that a horizontal line was obtained for a certain distance, moving from concave to convex, and conic sections is one of the simplest families, with this behaviour.

4. More Theory

Three pieces of information, Sections 4.1-4.3, are the platform for a theorem in Section 4.4.

4.1 Corresponding Retinal Points

Eq. 2 for a *fixed* nonzero H may be interpreted in terms of asymmetrically positioned corresponding points on two retinas (or two image planes, say $z_L^\perp = 1$, $z_R^\perp = 1$). Since H is fixed, then α_L is **only** a function of α_R irrespective of z_0 . Hence, a series of corresponding pairs (α_L, α_R) are obtained.

4.2 Abathic Distance

Abathic distance is, as usual, defined as that z_0 for which the horopter, the curve of corresponding rays is

a horizontal line in the (x, z) -plane, the fixation plane. It can be calculated from $1 - 0.5H\rho = 0$, cf. Appendix A, where $\rho = z_0/(b/2)$. This yields $z_0 = b/H$.

4.3 Associated Image Planes

The observant reader will have noticed we use x_L, x_R, z_L, z_R instead of $x_L^\perp, x_R^\perp, z_L^\perp, z_R^\perp$ as a kind of bookkeeping system for ray correspondences, but not for image formation itself. Call the directions x_L and x_R *associated directions*. They intersect at point Q (see Fig. 1).

Now, *imagine* that we insert extra image planes parallel to x_L, y_L -axes and x_R, y_R -axes. Such images would be blurry in lens-based optical systems, but we think of them as being sharp because we will only use them as analytical tools.

Def. These imagined image planes are called **associated image planes**.

They have two important properties: (a) Asymmetric ray correspondences by Eq. 2, Eq. 3 in (x, z) -coordinates, become *symmetric* and equidistant image points in associated image planes³, (b) the *extent to which associated image planes are nonfrontal* (=nonparallel to baseline AB) is a direct measure

³The serious reader should verify that this follows from the linear correspondence idea, the proof behind Eq. 1. Note also that we neglect y -coordinates when speaking of correspondences, i.e. we do not care about vertical disparities, here.

of perspective distortions accompanying the ray correspondences by Eq. 2, Eq. 3. (Property (b) is slightly abstract, and requires some effort to grasp.)

4.4 A Theorem

For usage in Section 5, we now prove:

Theorem: In symmetric fixation, the angle β between sections of associated image planes and actual image planes is constant and $\beta = \tan^{-1}(H/2)$.

Proof: For associated directions, by Eq. 2 a visual angle α_L corresponds to $\alpha_R = \pi - \alpha_L$. These directions intersect at Q in Fig. 1. We may also say (Fig. 1) that α_L corresponds to $-\alpha_L$ if replacing $\pi - \alpha_L$ with the acute angle. By construction, Eq. 2, this correspondence holds for **every** symmetric fixation, i.e., irrespective of z_0 . When α_L corresponds to $-\alpha_L$ we must be on the symmetry line PQ, due to symmetry. This means that the angles PAQ = α_L and angle PBQ = $-\alpha_L$ are constant when varying z_0 . The actual (left) image plane section \perp AP. Then $\beta = \pi/2 - \alpha_L$ is also constant, $\forall z_0$. The angle β can be calculated for a special case, namely for the abathic distance, whereby $\cot \beta = 2/H$.

4.5 Why Asymmetry?

For the purpose of measuring depth, the most natural level curves would be horizontal lines in the (x, z) -plane, i.e. in the fixation plane. Using ordinary disparity as a depth measure entails using V-M circles as level curves for depth, which for close range vision makes planar surfaces barrel-shaped. If using ellipses as level curves for depth instead, problems of this kind are alleviated. For that reason asymmetric stereo by Eq. 2 seems apriori preferable.

5. Designing Asymmetric Stereo

5.1 How to use Hering-Hillebrand deviation?

In symmetric, or fairly symmetric fixation, it makes sense using a fixed H , for relatively short fixation distances z_0 . However, when z_0 is so large that the fixation point is far behind the *abathic distance*, $z_0 > b/H$, there is something definitely odd about the idea of using a fixed H , both in the context of human and machine vision, clearly illustrated by Table 1.

In Table 1, we allude to human vision choosing the interpupillary distance, i.e. the baseline length, $b = 0.065$ m. The first 3 columns deal with fixation distance and related entities. For the ratio $\rho^{-1} = (b/2)/z_0$ there is an approximate equality $\rho^{-1} \approx \vartheta$, where ϑ is the angle⁴ shown in Fig. 3. When fixating at infinity $\vartheta = 0$. As proved by the theorem in Section 4.4, β is a *constant angle irrespective of fixation distance*⁵ and tells us *how many degrees the associated image*

⁴equal to half of the vergence angle.

⁵which is why the β -columns in Table 1 are constant.

Table 1: Positions of actual and associated image planes, as a function of H-H deviation.

$H = \frac{1}{10} \quad H = 0.05 \quad H = 0.01$					
z_0	ρ^{-1}	ϑ	β	β	β
0.20	0.163	0.161	0.05	0.025	0.005
0.40	0.081	0.081	0.05	0.025	0.005
0.80	0.041	0.041	0.05	0.025	0.005
2.0	0.016	0.016	0.05	0.025	0.005
6.0	0.005	0.005	0.05	0.025	0.005
∞	0	0	0.05	0.025	0.005
∞	0	0°	$\approx 3^\circ$	$\approx 1.5^\circ$	$\approx 0.3^\circ$

plane lies in front of the actual image plane, for a given chosen H , cf. columns 4,5,6 in the table. In general, the associated direction is at an angle ε with respect to the baseline:

$$\varepsilon = \tan^{-1}\left(\frac{H}{2}\right) - \tan^{-1}(\rho^{-1}) = \beta - \vartheta. \quad (4)$$

This angle is (except when $z_0 < 0.2$ m) very well approximated by

$$\varepsilon \approx \frac{H}{2} - \frac{b/2}{z_0} \quad (5)$$

The associated image plane is approximately 3° in front of the baseline, at $z_0 = 6$ m for $H = 0.10$, and roughly 1° in front of it at $z_0 = 6$ for $H = 0.05$. This is seen in Table 1, since $\varepsilon \approx 0.020$ radians $\approx 1.2^\circ$ in Eq. 5, when (see 5th column) $H = 0.05$, and so forth.

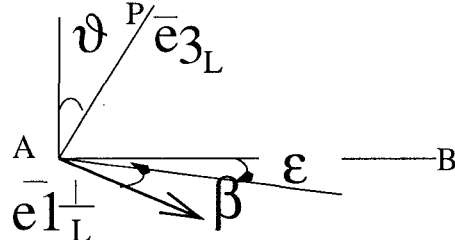


Figure 3: Involved angles. $\vartheta = \beta - \varepsilon$.

The built-in conflict between having a constant H and reasonable planarity perception is thus clear. For far away planar surfaces, it is odd to have an H that causes a larger concave distortion than the convex distortion caused by ordinary Vieth-Müller circles. At 6 m, $H = 0$ makes the image plane wind up 0.3° behind the baseline, but $H = 0.05$ makes the associated image plane wind up 1.5° in front of the baseline. The concave distortion caused by $H = 0.05$ is more than 5 times stronger than the convex distortion caused by $H = 0$, if measuring the strengths of the distortions by ε , i.e., how far away an associated image plane is bent away from the baseline.

5.2 How to modify H

For machine vision, we support the view that it is practical to use several sets of Hering-Hillebrand de-

viations. The human horopter related H-H deviation, i.e. $H \in [0.05, 0.13]$ is practical for *short-range vision*, say at distances $z_0 < 1$ m, whereas lower values should be used farther away. These lower values we call H^* instead of H , below.

For human vision, monocular empirical factors to distance perception, such as innervations to *accommodative* musculature, *perspective*, *motion parallax*, *aerial perspective* etc. can potentially be used to modify H into H^* , for longer distances. It is known that the apparent fronto-parallel plane⁶ also is well-approximated by conic sections with a Hering-Hillebrand deviation around $H^* \approx 0.01$ at 6m according to Ogle (1964,p.43). However, Ogle was not in position to conclude that $H^* \neq H$, because measurements using the subjective direction or fusion criteria for the longitudinal horopter could not be made beyond 76 cm, with his apparatus, [2].

In machine vision, it should be noted that if we just want to solve the problem about variable Hering-Hillebrand deviations, in a crude fashion, the simplest alternative would be to follow the recipe: Fixate on various points over a wide panorama (by neck rotations of binocular system) in a scene, and if crudely calculated disparities, using $H^* \approx 0$, tend to be all positive, we are fixating at a rather distant point, whence it follows that the ratio z_0/b is high. In that case, use $H^* \approx 0$ instead of H for final disparity map.

6. Asymmetric Stereo using H

Here, we will investigate the topic of asymmetric stereo and depth measurements from horizontal disparity more closely. First, note that we may redefine disparity for close-range depth perception, using the Hering-Hillebrand deviation, e.g., in the following way:

$$d_{new} = \text{Const} \cdot (F(t_L) - t_R) \quad (6)$$

$$F(t_L) = t_L / (1 - H \cdot t_L) \quad (7)$$

where d_{new} means *new disparity* measure, and $t_L = \tan \alpha_L$, $t_R = \tan \alpha_R$. The constant is a camera dependent constant (pixels/m) for converting disparity into pixel units. The difference between traditional disparity d and d_{new} is in our case:

$$d_{new} - d = \text{Const} \cdot (F(t_L) - t_L) \quad (8)$$

which can be shown to grow quadratically with distance from the image origin (=principal point).

⁶The apparent fronto-parallel plane is not an horopter in the sense of the subjective direction or fusion criteria, but can be determined by the *same* horopter apparatus used for the longitudinal horopter, employing movable vertical rods.

In the experiment reported below, cameras are fixating a nearby point in symmetric fixation. We wanted to have a *reference experiment* of exactly the same scene and almost the same camera-setup, where no perspective distortions of planar surfaces should take place, implying parallel binocular geometry.

The *reference experiment* is supposed to be *parallel binocular geometry* with the **same** point of fixation. This can be done by using slanted rays to the midpoint of the image, so-called slanted primary lines of sight. (The point of fixation is the intersection of the primary lines of sight.)

For this purpose, the authors constructed a *flexible-body CCD camera*, the functionality of which was reported in Francisco & Bergholm (1995). We called the binocular geometry arising from having parallel optical axes but slanting primary lines of sight: *skewed parallel geometry*. In the thirties, cf. [8], stereo by horizontally moving a flexible-body camera into new positions, was called *keystone-free* camera movements.

6.1 The Stereo Algorithm

We used a quite raw stereo correspondence algorithm, in order to have a clear understanding of the path from measurements to results. We preferred a simple transparent stereo matching algorithm (prone to some crude mismatches occasionally) to a more complex one, containing, e.g., the smoothness constraint, cf. [6], which, of course, would tend to decrease the number of mismatches.

The right image was shifted, in the horizontal direction, pixel by pixel for about 90 steps, from $\Delta x = -10$ to $\Delta x = 80$, creating internally a stack of 90 right images, and noting correspondence maxima⁷, thereby creating a (horizontal) *disparity* image.

6.2 Experimental Results

The experiment was designed to simulate the conditions of vision close to the near point of the eye, i.e., a low ratio $z_0 : b/2$. The baseline was $b = 1$ m, and focal length $F=12.5$ mm, and field of view around $20^\circ - 25^\circ$. The images captured (symmetric fixation) are shown in Fig. 1,2. Cameras were not moved when doing the reference experiment, just rotated into parallel geometry, plus camera-body shifts for obtaining the same

⁷The 90 shifted images were divided into two image stacks, one for positive shifts, and one for negative shifts, and each of them was compared with the left image by a correspondence operator (= correlation coefficient in a 7 by 7 window), cf. Francisco (1994, p.79). In each of the two stacks of correspondence images the highest local maxima, *forming a vertical path for each pixel*, were noted together with the shift Δx at which each maximum occurred, in the stack, which becomes a (horizontal) *disparity* image. In the experiments, we only dealt with the positive disparity image, since we focused our attention on a planar surface with disparities in the interval [50, 70] pixels.

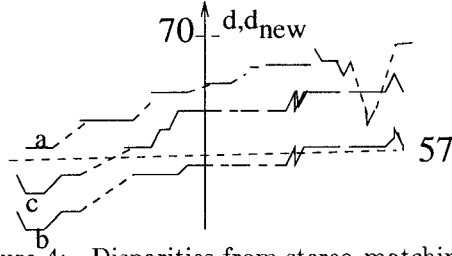


Figure 4: Disparities from stereo matching on a real image: a= (skewed) parallel geometry, b= convergent geometry, ordinary disparity, c= new disparity measure using $H = 0.10$. Disparities differing by more than ± 7 pixels from moving average of disparities were discarded (=mismatches). Omission of disparity data indicated by dotted lines, above. $d, d_{new} \in [53, 65]$.

fixation point. Slight vignetting and radial distortion effects affect the images in the reference experiment. We used $H = 0.10$ in the vergence geometry experiment, Eq. 7, since it lies in the middle of the interval $H \in [0.05, 0.13]$ from empirical data in Ogle (1964).

In the scene there are a number of planar surfaces. The periodic pattern upon which the cameras are fixating is not ideal for illustrating measurement results, because of matching problems for periodic patterns. Concentrating on a planar surface of a box, to the left, horizontal slices of disparity measurements were gathered over that surface, see Fig. 4. It turns out that trace a (= parallel geometry), yields a reasonably correct slope, trace b (=convergent geometry with $H = 0$) yields quite incorrect slope, and trace c (=convergent geometry with $H = 0.10$) yields almost the correct slope of the planar patch section. (We expect an intermediate case between the two extremes, here.) Normally, planar surfaces are made barrel-shaped by ordinary disparities in convergent geometry. However, if the planar surface is not so extended, the effect is mainly that of changing slope, and a barely visible ‘barrel-bending effect’.

7. Summing Up

This article (a) motivates mathematically the elliptical-like horopter of human vision, (b) shows the need for variable Hering-Hillebrand deviation H over fixation distance, from an efficiency point of view for depth perception, (c) suggests the use of H for an alternative disparity measure in machine vision.

Future Work

Next step towards a deeper analysis of the human horopter must involve investigations aimed at answering: To what extent is the human longitudinal horopter a result of asymmetries in the ocular system as discussed for example by Halldén (1956), or retinal asymmetries?

Also, it is a pity that the horopter apparatus of Ames and Ogle was limited to a fixation distance of 1 m, for the subjective direction criterion. It would be quite interesting to have measurements of H for distances beyond 1 m, applying this horopter criterion. If such experiments have been performed, the authors would be eager to learn to know about them.

References

- [1] Ogle, K.N., “An Analytical Treatment of the Longitudinal Horopter : Its Measurement and Application to Related Phenomena, Especially to the Relative Size and Shape of the Ocular Images”, *J. of Opt. Soc. Am.*, Vol. 22, No.12, pp.665-728, Dec. 1932.
- [2] Ames, A.Jr., Ogle, K.N., Gliddon, G.H., “Corresponding Retinal Points, the Horopter and the Size and Shape of the Ocular Images”, *J.O.S.A.*, Vol.22, pp. 538-575, 1932.
- [3] Ogle, K.N., **Researches in Binocular Vision**, reprinted from 1950, Hafner Publ. Company, London, New York, 1964.
- [4] Fry, G.A., “Binocular Vision”, in **Foundation of Sensory Science**, (Ed.) Dawson, W.W., Springer Verlag, Chapter 8, 1984.
- [5] Francisco, A., Bergholm, F., “On the importance of being asymmetric in stereopsis”, in *Proc. of Scandinavian Conference on Image Analysis*, pp. 77-86, Uppsala, Sweden, June 1995.
- [6] Marr, D., Poggio, T., “A Computational Theory of Human Stereo Vision”, *Proc. of the Royal Society of London B*, Vol.204, pp.301-328, 1979.
- [7] Okoshi, T., **Three-dimensional Imaging Techniques**, Academic Press New York, London, ISBN 0-12-525250-1, 1976.
- [8] Halldén, U., “An Optical Explanation of Hering-Hillebrand’s Horopter Deviation”, *Arch. Ophth.* 55:pp.830-835, 1956.
- [9] Francisco, A., “Active Structure Acquisition by Continuous Fixation Movements”, Ph.D Thesis, ISRN KTH/NA/P-94/17-SE, KTH, Stockholm, Sweden, 1994.

App. A: Ogle’s family of conics.

Let $\rho = z_0/(b/2)$. Referring to the conic $A^{(H)}x^2 + B^{(H)}z^2 + D^{(H)}z = E^{(H)}$:

$$A^{(H)} = 1 - \frac{1}{2}H\rho \quad (9)$$

$$B^{(H)} = 1 + \frac{1}{2}H\rho^{-1} \quad (10)$$

$$D^{(H)} = \frac{b}{2}(\rho - \rho^{-1} + H) \quad (11)$$

$E^{(H)} = (b/2)^2 A^{(H)}$. For a fixed baseline b , the family is a function of z_0 (ρ) and H .

App. B: Conics from Linear Correspondence

For symmetric fixation,

$$\begin{pmatrix} x \\ z \end{pmatrix} = \begin{pmatrix} c & C \\ s & S \end{pmatrix} \begin{pmatrix} x_L \\ z_L \end{pmatrix} + \begin{pmatrix} -b/2 \\ 0 \end{pmatrix} \quad (12)$$

$$\begin{pmatrix} x \\ z \end{pmatrix} = \begin{pmatrix} c & -C \\ -s & S \end{pmatrix} \begin{pmatrix} x_R \\ z_R \end{pmatrix} + \begin{pmatrix} b/2 \\ 0 \end{pmatrix} \quad (13)$$

$$(C, S) = (\cos \theta_L, \sin \theta_L) = k \cdot (b/2, z_0) \quad (14)$$

$$(c, s) = (\cos \gamma, \sin \gamma) \quad (15)$$

and the point conic is determined by Eq. 1, which yields: $Ax^2 + Bz^2 - Dz = E \iff$

$$-sSx^2 + Ccz^2 - (Cs + cS)\frac{b}{2}z = -sS\left(\frac{b}{2}\right)^2 \quad (16)$$

There is no difference between this conics family and that in App. A. They are **2 alternative** descriptions.